Jurnal Teknologi

Full Paper

BREAKDOWN OF GLUCOMANNAN ISOLATED FROM *AMORPHOPHALLUS MUELLERI*: OPTIMIZATION OF ENZYMATIC HYDROLYSIS CONDITIONS

Muhammad Imran Ishak[a], Roshanida A. Rahman[a,b]*, Mohammad Nashriq Jailani[a], Nur Aizura Mat Alewi[a], Rosli Md. Illias[a,b], Nardiah Rizwana Jaafar[a], Kazuhito Fujiyama[c], Ni Nyoman Tri Puspaningsih[d], Mohd Faizal Ahmad Jaafar[e], Azura Aziz[e]

[a]Department of Bioprocess and Polymer Engineering, Faculty of Chemical and Energy Engineering, Universiti Teknologi Malaysia, 81310 UTM Johor Bahru, Johor, Malaysia
[b]Innovation Centre in Agritechnology for Advanced Bioprocessing, Universiti Teknologi Malaysia, 84600 Pagoh, Johor, Malaysia
[c]International Center for Biotechnology, The University of Osaka, 2-1 Yamadaoka, Suita 565-0871, Osaka, Japan
[d]Faculty of Science and Technology, Universitas Airlangga, Surabaya, 60115 East Java, Indonesia
[e]Ladang Konjak Sdn Bhd, 1-28-10, M-City, 326, Jalan Ampang, 50450 Kuala Lumpur, Malaysia

Article history
Received
17 September 2025
Received in revised form
25 November 2025
Accepted
8 January 2026
Published Online
30 April 2026

*Corresponding author
r-anida@utm.my

Graphical abstract

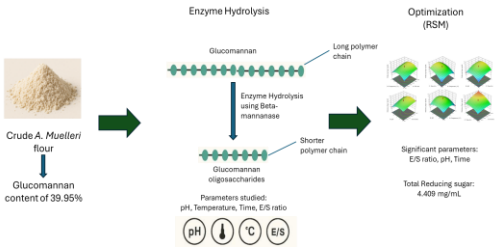

Abstract

The enzymatic breakdown of glucomannan from *Amorphophallus muelleri* (*A. muelleri*), a species related to konjac, using β-mannanase, is a promising approach to produce functional oligosaccharides. This enzymatic breakdown success depends critically on the operating parameters. Understanding their interactions is essential to optimize the hydrolysis process and product yield. This study utilized Response Surface Methodology (RSM) to investigate the effects of reaction time, pH, temperature, and enzyme-substrate (E/S) ratio on the hydrolysis, with the aim of maximizing the total reducing sugar (TRS) production. The results indicated that the E/S ratio, pH, and reaction time significantly affected hydrolysis efficiency ($p < 0.05$), while temperature had an insignificant impact ($p > 0.05$). The ideal conditions were determined to be an E/S ratio of 1:500 (v/v), pH 5.7, 41.5 °C, and 5 h, resulting in a TRS yield of 4.409 ± 0.030 mg/mL, with a difference of merely 1.46% from the expected values. This study demonstrates the viability of *A. muelleri* as a sustainable resource for oligosaccharides production and confirms that enzymatic hydrolysis coupled with RSM is an effective approach for process optimization.

Keywords: *Amorphophallus muelleri*, konjac, glucomannan, enzymatic hydrolysis, Response Surface Methodology

Abstrak

Penguraian enzimatik glukomanan daripada *Amorphophallus muelleri* (*A. muelleri*), satu spesies yang berkait dengan konjac, menggunakan β-mannanase adalah satu pendekatan yang menjanjikan untuk menghasilkan

oligosakarida berfungsi. Kejayaan biopenukaran ini sangat bergantung pada parameter operasi. Memahami interaksi parameter-parameter ini adalah penting untuk mengoptimumkan proses hidrolisis dan hasil produk. Kajian ini menggunakan Response Surface Methodology (RSM) untuk menyiasat kesan masa, pH, suhu, dan nisbah enzim-substrat (E/S) terhadap hidrolisis, bertujuan untuk memaksimumkan penghasilan jumlah gula penurun (TRS). Keputusan menunjukkan bahawa nisbah E/S, pH, dan masa tindak balas memberi kesan yang signifikan terhadap kecekapan hidrolisis ($p < 0.05$), manakala suhu mempunyai kesan yang tidak signifikan ($p > 0.05$). Keadaan ideal dikenal pasti adalah nisbah E/S 1:500 (v/v), pH 5.7, 41.5 °C, dan 5 jam, menghasilkan TRS sebanyak 4.409 ± 0.030 mg/mL, dengan perbezaan hanya 1.46% daripada nilai yang dijangkakan. Kajian ini menunjukkan kebolehlaksanaan *A. muelleri* sebagai sumber mampan untuk penghasilan oligosakarida dan mengesahkan bahawa hidrolisis enzimatik yang digabungkan dengan RSM adalah pendekatan yang berkesan untuk pengoptimuman proses.

Kata kunci: *Amorphophallus muelleri*, konjak, glukomanan, enzim hidrolisis, Response Surface Methodology

1.0 INTRODUCTION

Glucomannan is a polysaccharide that is known for its high molecular weight and water-soluble properties, primarily extracted from the genus *Amorphophallus*. This genus has been extensively studied for its exceptional nutritional and therapeutic properties. *Amorphophallus konjac, Amorphophallus muelleri, Amorphophallus krausei, Amorphophallus kachiensis, Amorphophallus bulbifer, Amorphophallus xiei, and Amorphophallus corrugatus* are examples of glucomannan sources, where each species contains varying glucomannan content depending on the collection area [1]. *A. konjac* has been recorded to have the highest glucomannan content (40-70%), followed by *A. muelleri* (60-68%), *A. krausei* (52-57%), *A. kachiensis* (55%), *A. bulbifer* (42%), *A. xiei* (40%), and *A. corrugatus* (35.41%) [2]. Despite *A. muelleri's* notable glucomannan content, research on this species remains limited compared to *A. konjac*, which is mainly cultivated in China and has been extensively studied for glucomannan extraction and degradation [3]. *A. muelleri,* currently cultivated in Southeast Asia, is a sustainable yet underutilized source of glucomannan and thus warrants further scientific investigation [4].

Structurally, glucomannan is composed of β-(1,4)-linked mannose and glucose units in a molar ratio of 1.5:1. This composition gives rise to four different linkages: mannose to mannose, mannose to glucose, glucose to mannose, and glucose to glucose [5]. Glucomannan can act as a prebiotic by selectively enhancing the growth of beneficial gut microbiota such as *Bifidobacterium* and *Lactobacillus* [6]. Fermentation of glucomannan by commensal gut bacteria produces short-chain fatty acids (SCFAs), including acetate, propionate, and butyrate. These SCFAs play pivotal roles in maintaining colonic health, enhancing gut barrier integrity, and exerting systemic anti-inflammatory effects [7, 8]. Given these advantages, glucomannan has attracted attention as a functional component in low-calorie food formulations, dietary supplements, and nutraceuticals.

Despite its health benefits, the practical application of native glucomannan is limited by its elevated viscosity and substantial molecular structure, which inhibit effective digestion and absorption in the upper gastrointestinal tract [9]. These characteristics not only reduce its bioavailability but also diminish its prebiotic efficiency, as intact glucomannan may undergo only partial fermentation in the distal colon. To address these limitations, enzymatic hydrolysis is used to degrade glucomannan into glucomannan oligosaccharides (GMOs), which offer improved solubility, reduced viscosity, and enhanced fermentability. GMOs preserve the advantageous characteristics of their parent polymer while providing enhanced functionality. Their reduced molecule size enhances microbial utilisation, resulting in increased SCFAs synthesis and a more significant prebiotic effect [10]. These characteristics make GMOs a better alternative to native glucomannan in functional food and medicinal applications.

Several depolymerization techniques can produce GMOs, but they vary greatly in efficiency and safety. Chemical methods, such as acid degradation and oxidative degradation, are effective at cleaving the β-1,4-linkages in glucomannan but suffer from major drawbacks. These harsh processes can lead to over-hydrolysis and the formation of undesirable or even toxic byproducts, such as furfural and formic acid, making them less suitable for food and pharmaceutical applications [11]. On the other hand, enzymatic hydrolysis provides a more sustainable and regulated method for producing GMOs, functioning at mild

conditions while reducing the destruction of bioactive constituents [12]. β-Mannanase is a highly effective enzyme for the depolymerization of glucomannan, as they specifically cleave β-(1,4)-glycosidic links in the glucomannan backbone, producing mannobiose and mannose as significant products of hydrolysis [13]. Tripetch *et al*. [14] and Pomsang *et al*. [15] showed in their study that endo-β-Mannanase was able to successfully hydrolyse konjac glucomannan into glucomannan oligosaccharides. Based on the findings of these studies, β-Mannanase has the potential to effectively hydrolyse glucomannan from *A. muellleri.*

Nevertheless, the efficacy of enzymatic hydrolysis is significantly influenced by key reaction parameters, including the enzyme-substrate ratio, pH, temperature, and incubation time [16]. Suboptimal conditions may lead to incomplete and inefficient hydrolysis that yields high-molecular-weight fragments with low solubility. Consequently, optimizing these operating parameters is critical for enhancing and maximizing the yield of GMOs derived from *A. muellleri*. Subsequently, given that *A. muelleri* belongs to the same genus as *A. konjac*, a species widely recognized for its extensive applications and benefits, it holds promise to produce comparable or even greater quantities of high-quality GMOs. This taxonomic relationship highlights the importance of systematically examining its hydrolysis behavior and identifying conditions that promote efficient oligosaccharide production. Accordingly, this study aims to investigate the enzymatic hydrolysis of *A. muelleri* glucomannan using β-mannanase to generate GMOs by assessing the impact of critical hydrolysis parameters such as enzyme-substrate ratio, pH, temperature, and reaction time on the total reducing sugar (TRS) yields To achieve this, Response Surface Methodology (RSM) is employed as it enables a comprehensive evaluation of both the individual and interactive influences of these four critical parameters. This is essential for building a predictive model and identifying the optimal conditions that maximize GMOs production. Overall, the insights gained from this optimization will be essential for developing a scalable and efficient bioprocess, thereby unlocking the potential of *A. muelleri* glucomannan as a valuable source of functional oligosaccharides for industrial applications.

2.0 METHODOLOGY

2.1 Materials and Chemicals

Crude *A. muelleri* flour was purchased from Ladang Konjac Sdn. Bhd. (Malaysia). β-mannanase was purchased from Beijing Huawei Ruike Chemical Co., Ltd (Beijing, China). D-(+)-glucose, D-(+)-Mannose, bovine serum albumin (BSA), Bradford reagent, dinitrosalicylic acid, sodium hydroxide, sodium potassium tartrate, citric acid monohydrate, disodium hydrogen phosphate, sulphuric acid, formic acid, and hydrochloric acid were purchased from Sigma Chemical Co. (St. Louis, MO).

2.2 Proximate Analysis of *Amorphophallus muelleri* Flour

The proximate analysis for protein, moisture, crude fibre, fat, and ash content of *A. muelleri* flour was calculated using methods following AOAC (1995) [17]. The carbohydrate content was determined by subtracting with total of protein, moisture, crude fibre, fat, and ash content from the weight of the sample (100 g).

2.3 Glucomannan Content of *Amorphophallus muelleri* flour

Crude *A. muelleri* flour's glucomannan content was determined using the procedure reported by Chua *et al*. [18]. Approximately 0.2 g of *A. muelleri* flour was added to 50 mL of 0.1 M formic acid sodium hydroxide buffer in a volumetric flask, followed by centrifugation at 4500×g, 40 min, 25 °C. In boiling water, 2.5 mL of sulphuric acid (3 M) was added to 5 mL of the obtained solution, stirred, and hydrolyzed for 90 min. The sample was allowed to cool to room temperature before 2.5 mL of sodium hydroxide (6 M) was added. Next, 15 mL of distilled water was added to the solution to make up glucomannan hydrolytes before the DNS colorimetric assay was performed to determine the glucomannan content in *A. muelleri* flour. Absorbance was measured at 540 nm, and a glucose standard curve (absorbance against sugar concentration) was used to determine glucose concentration. The glucomannan content was determined by the following Equation (1):

$$\text{GM content (\%)} = [5000f(5T-T_0)] \div m \quad (1)$$

where f is the correction factor, T is the glucose concentration of glucomannan hydrolysate (mg), T_0 is the glucose concentration of glucomannan sample solution (mg), and m is the mass of *A. muelleri* flour (mg).

2.4 Protein Concentration and Enzyme Activity

The Bradford method [19] was used to determine the protein content of the enzyme using bovine serum albumin (BSA) as a standard. An allocated amount of 5 µL of enzymes was transferred into labelled tubes, and 5 µL of distilled water was used as a blank. Each tube was added with 250 µL of 1x Bradford reagent, mixed well, and incubated for 5 min at room temperature. A UV-VIS spectrometer was used to measure the absorbance of each sample at 595 nm. The absorbance reading versus standard BSA concentration at 0.5, 1.0, 2.0, 3.0, 4.0, 5.0, 6.0, 7.0, and 8.0 mg/mL was plotted to prepare a standard

curve. Protein concentration was calculated according to Equation (2):

$$\text{Protein concentration (mg/mL)} = A_{595} \div C \quad (2)$$

where, A_{595} is the absorbance of the sample at 595nm, and C is the slope of the BSA standard curve.

Enzyme activity was determined using the DNS approach [20], where 2 µL of enzyme solution (100 mg/mL) was added to 100 µL of glucomannan solution (10 mg/mL) as a substrate and followed by addition of 898 µL citric acid buffer (pH 5.0) to make up the 1 mL of reaction solution. The mixture was incubated at 45 °C for 30 min. The mixture was centrifuged, and 250 µL of supernatant was added to 250 µL of distilled water before adding 500 µL of DNS reagents. The DNS mixture was boiled for 5 min, then cooled for 5 min in cold water. Absorbance of the DNS mixture (100 µL) was observed using a UV-VIS spectrometer at 540 nm. The mannose standard curve was used to calculate the activity. The unit (U) of β-mannanase was defined as the quantity of enzyme needed to release 1 µmol of mannose per minute. The enzyme activity and specific activity were calculated using Equation (3) and Equation (4) as shown below:

$$\text{Enzyme activity, U/mL} = (f \times V_a) \div (V_b \times t \times V_c) \quad (3)$$

$$f = \text{Enzyme Activity (U/mL)} \div \text{Protein Concentration (mg/mL)} \quad (4)$$

f is the µmol of mannose released (Absorbance/slope of the standard curve), t is the reaction time, V_a= total reaction volume (mL), V_b is the enzyme's volume (mL), and V_c is the volume in the cuvette (mL).

2.5 Screening of Enzyme Hydrolysis Parameters by OFAT Methods

Four key parameters (i.e.: time, enzyme-substrate (E/S) ratio, pH, and temperature) were screened. To prepare the substrate, 0.5 g of crude *A. muelleri* flour was added to 50 mL of 50 mM $NaHPO_4$-citric acid buffer adjusted to various pH levels (pH 3 to 7), yielding a 1% *A. muelleri* glucomannan (AGM) solution. ß-mannanase was added at enzyme substrate (E/S) ratio (v/v) ranging from 1:2500 to 1:300. The mixture was then incubated in a water bath shaker, with reaction times ranging from 1 to 5 h and temperatures spanning 30 to 70 °C. Upon completion of the hydrolysis, the sample was centrifuged at 4,500×g for 30 min, and the resulting supernatant was analyzed for total reducing sugar (TRS) content using the DNS method [20].

2.6 Optimization of Hydrolysis Parameters using Response Surface Methodology (RSM)

Operating conditions identified during the initial screening were further optimized using RSM based on Box-Behnken Design (BBD), where the independent variables were the E/S ratio (A), pH (B), reaction time (C), and temperature (D). Reducing sugar (Y) was selected as the response variable. The BBD consisted of 29 experimental runs, including five center points. The experimental data fit the following second-order polynomial Equation (5):

$$Y = b_0 + \sum_{i=1}^{4} b_i X_i + \sum_{i=1}^{4} b_{ii} X_i^{\,2} + \sum_{i=1}^{3} \sum_{j=i+1}^{4} b_{ij} X_i X_j \quad (5)$$

where Y is the dependent variable (Total Reducing Sugar), b_0, b_i, b_{ii}, and b_{ij} are coefficients estimated by the model, X_i, X_j are levels of the independent variables. They represent, respectively, the response's linear, quadratic, and cross product impacts of the A, B, C, and D components.

2.7 Statistical Analysis

All data are reported as the average amounts of at least three replicate samples. The data are presented as the mean ± standard deviation of OFAT screening (Section 2.5). A significant difference between the means was determined by a two-way ANOVA, Tukey multiple comparison test. The different letters were used to indicate that the differences between data were statistically significant ($p < 0.05$) The calculations were performed using GraphPad Prism (GraphPad Software, LLC, San Diego, California, USA).

3.0 RESULTS AND DISCUSSION

3.1 Characterization of Crude *A. muelleri* and β-mannanase

The proximate composition of crude *A. muelleri* is summarized in Table 1. Carbohydrates were identified as the predominant constituent, accounting for 71.9 g/100 g of total dry matter, which supports the suitability of *A. muelleri* as a potential glucomannan source. It was noted that the carbohydrate content was slightly lower than the 73-80% range reported by Nur'aini *et al.* [21], a variation that may reflect differences in processing methods, or environmental conditions. Notably, even with the high carbohydrate content, only a fraction corresponds to glucomannan, as it also contains other carbohydrates, such as starch [23]. This distinction underscores the need for further compositional analysis to accurately determine the glucomannan yield. In this study, the glucomannan content of *A. muelleri* flour was 33.95%. Pambudi *et al.* [1] documented diverse glucomannan concentrations across several *Amorphophallus* species, including *A. muelleri* (60.16-68.93%), *A. krausei* (52.14-57.76%), *A. kachiensis* (51.52%), *A. bulbifer* (45.83%), *A. Xiei* (40.60%), and *A. corrugatus* (35.41%). These were categorized into low (16%), moderate (22–24%), and high (32–42%) glucomannan groups [1]. Based on this classification,

the glucomannan content obtained in the present study falls within the high category, reaffirming its suitability as a glucomannan source. Enzyme activity of β-mannanase was measured at 137.65 U/mL, with protein content of 2.18 mg/mL. The specific enzyme activity was determined to be 63.14 U/mg based on its protein content and enzyme activity. This activity demonstrates the catalytic efficiency of β-mannanase, quantifying enzyme units per milligram of protein, and acts as an indicator of enzyme purity and functionality.

Table 1 Proximate composition of *A. muelleri* flour

Composition	Content (g/100g)
Carbohydrate	71.9
Water	10.9
Protein	8.8
Ash	5.0
Crude Fiber	3.0
Lipid	0.4

3.2 Effect of Reaction Time

The results of glucomannan hydrolysis by the enzyme at different reaction times are shown in Figure 1. The reaction time was set from 1 to 5 h, while other parameters were set to 40 °C, enzyme substrate (E/S) ratio 1:1000 (v/v), and pH 5. The total reducing sugar (TRS) increased from 1.253 mg/mL to 3.498 mg/mL within the first 4 h, indicating that the enzyme has successfully hydrolyzed the glucomannan. The statistically significant ($p < 0.05$) between the time intervals of 1 to 3 h imply that the reaction is developing at a noticeable rate during this time. There was an insignificant increase after 4 h, which is from 3.498 mg/mL to 3.558 mg/mL, as indicated by the bars at 4 h and 5 h having the same letter A ($p > 0.05$). Anggela *et al*. [22] found that increasing reaction time enhanced oligosaccharide yields up to an optimal point, after which yields plateaued, which correlates with observations of reducing sugars stabilizing beyond 4 h. At high substrate concentrations, enzyme active sites become saturated. This causes the reaction rate and TRS production to plateau, regardless of additional substrate. Li *et al*. [23] highlighted that during enzyme hydrolysis, the initial rapid production of reducing sugar can slow down as substrate binds to the enzyme surface, masking the active site and reducing the enzyme hydrolysis. These trends occur because the enzyme has fully hydrolyzed with available substrate, which limits its activity. The kinetics of enzymatic hydrolysis are influenced by substrate concentration, which can directly affect reducing sugar yield [24]. Because of that, 4 h has been chosen as the optimum condition. 3 h, 4 h, and 5 h were chosen as low, medium, and high for RSM, respectively.

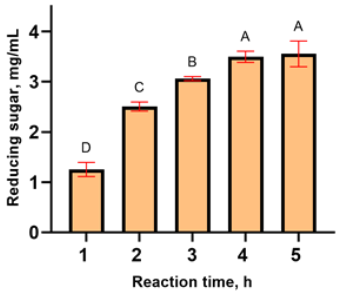

Figure 1 Effect of reaction time on total reducing sugar production. The different letters (A, B, C, and D) above the bars indicate the statistical significance ($p < 0.05$) between samples

3.3 Effect of pH

The results of glucomannan hydrolysis by the enzyme at different pH levels are shown in Figure 2.

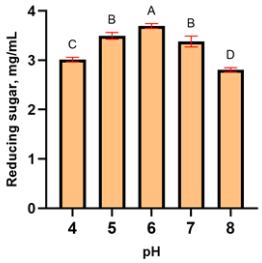

Figure 2 Effect of pH on total reducing sugar production. The letters (A, B, C, and D) above the bars indicate bars indicate the statistical significance ($p < 0.05$) between samples

The pH was set from 4 to 8, while other parameters were set at 40 °C, E/S ratio 1:1000 (v/v), and 4 h. The highest reducing sugar production occurs at pH 6 with 3.692 mg/mL, and this pH is considered the optimum condition for the hydrolysis of glucomannan. As the pH decreases from 6 to 4, there is a gradual decrease in TRS production from 3.692 mg/mL to 3.012 mg/mL, which indicates the enzyme's activity is reduced in more acidic conditions. Similarly, as the pH increases from 6 to 8, there is a decrease in reducing sugar production to 2.806 mg/mL, which shows that the enzyme's activity is also reduced in more alkaline conditions. Enzyme usually exhibits specific activity ranges, with pH significantly influencing their structural stability and catalytic efficiency, where suboptimal conditions will cause a reduction in degradation products [25]. Anggela *et al*. [22] mention that the stability and activity of ß-mannanase are usually optimum in a low acidic range, which is from pH 5 – 6. Under these optimal pH conditions, the enzyme maintains its structural integrity and catalytic efficiency, allowing it to effectively cleave the mannan backbone of

glucomannan into oligosaccharides. Because of that, it can be concluded that ß-mannanase shows specific preferences at pH 6, as it produced the highest amount of TRS. Subsequently, pH 5, pH 6, and pH 7 were chosen as low, medium, and high pH conditions for RSM, respectively.

3.4 Effect of Temperature

The temperature was varied from 30 to 70 °C, while other parameters were maintained (pH 6, E/S ratio 1:1000 (v/v), and reaction time of 4 h). As shown in Figure 3, the response followed the characteristic temperature-activity profile of enzymes. The highest TRS production was achieved at 40 °C and 50 °C, yielding 3.555 mg/mL and 3.540 mg/ mL, respectively, with no significant difference between the results ($p > 0.05$). This suggests that the enzyme exhibits optimal catalytic activity within this temperature range, where molecular collisions are enhanced without compromising structural stability. Beyond 50 °C, the production of TRS significantly decreased, reflecting reduced enzyme activity likely caused by thermal inactivation or the early onset of denaturation. Furthermore, lower temperatures also resulted in a declined of enzyme activity as the amount of reducing sugar at 30 °C was recorded to be 3.192 mg/mL, significantly lower than at 40 °C ($p < 0.05$). This trend aligned with established enzyme kinetics, in which activity increases with temperature until excessive thermal energy leads to enzyme inactivation or denaturation [26]. These findings are consistent with previous studies by Anggela *et al*. [22] who reported an optimal temperature of 37 °C, while Ariestanti *et al*. [8] observed a maximum at 48 °C, both slightly below the 50 °C threshold identified. Based on these results, temperatures set at 30, 40, and 50 °C were chosen as the low, medium, and high levels, respectively, for RSM optimization.

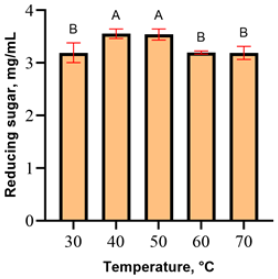

Figure 3 Effect of temperature on total reducing sugar production. The letters (A and B) indicate the statistical significance ($p < 0.05$) between samples

3.5 Effect of Enzyme-Substrate Ratio

E/S ratio was set at 1:2000 (v/v), 1:1500 (v/v), 1:1000 (v/v), 1:500 (v/v), 1:400 (v/v), and 1:300 (v/v) while other parameters are set to pH 6, 40 °C, and 4 h. Figure 4 shows that as the increase of E/S ratio increases, the production of reducing sugar increases generally, especially from 1:200 (v/v) to 1:500 (v/v), 2.502 mg/mL to 3.868 mg/mL, which shows a significant difference ($p < 0.05$). The production of reducing sugar showed insignificant differences ($p > 0.05$) at 1:500 (v/v), 1:400 (v/v) and 1:300 (v/v) with TRS of 3.868 mg/mL, 3.872 mg/mL and 3.879 mg/mL, respectively, suggesting that the reaction has reached a saturation point where increasing the amount of enzyme does not significantly increase the production of reducing sugar. Sui *et al*. [27] emphasized that after increasing enzyme loading to specific thresholds, the product of hydrolysis showed insignificant improvement. E/S ratios of 1:1000 (v/v), 1:571 (v/v), and 1:400 (v/v) were chosen as low, medium, and high pH conditions for RSM, respectively. As RSM cannot process inputs in ratio format, their decimal equivalents were used: 1:1000 = 0.001, 1:571 = 0.00175, and 1:400 = 0.0025.

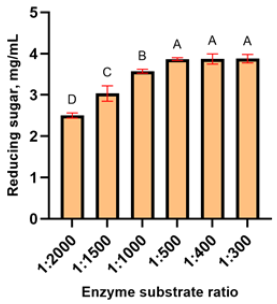

Figure 4 Effect of enzyme-substrate ratio on total reducing sugar production. The different letters (A, B, C, and D) above the bars indicate the statistical significance ($p < 0.05$) between samples

3.6 Response Surface Optimization

Based on OFAT screening results, the highest TRS yield (3.868 mg/mL) was achieved at pH 6, 40 °C, with E/S ratio of 1:500 (v/v), and reaction time of 4 h. The OFAT method has its limitations, as it is unable to evaluate interactions between variables that may skew interpretations and yield suboptimal results [28]. Alternatively, RSM offers a more robust approach, as it enables the simultaneous evaluation of multiple variables and their interactive effects, thereby improving reducing experimental variability [29, 30]. Using the parameters identified in the OFAT screening (reaction time, 3–5 h; pH 5–7; temperature 30–50 °C; E/S ratio 1:1000–1:400) a Box–Behnken design (BBD) was employed to systematically explore optimization conditions. The design consisted of 29 sets of experiments, including 5 center points (Table 2). Table 3 summarizes the ANOVA results.

Table 2 Optimization of TRS production through enzyme hydrolysis using Box-Behnken Design

Run	Independent Variables				Response: Reducing sugar	
	A (v/v)	B (pH)	C (h)	D (°C)	Predicted (mg/mL)	Actual (mg/mL)
1	1:400	6	4	30	3.725	3.635 ± 0.021
2	1:571	7	4	30	3.211	3.307 ± 0.022
3	1:571	7	4	50	3.079	3.107 ± 0.032
4	1:571	6	3	50	3.069	3.099 ± 0.021
5	1:571	6	5	40	3.584	3.623 ± 0.010
6	1:571	7	4	40	3.706	3.741 ± 0.113
7	1:571	6	5	50	3.738	3.836 ± 0.042
8	1:571	6	3	30	3.165	3.157 ± 0.022
9	1:571	5	4	50	3.483	3.433 ± 0.017
10	1:1000	7	4	40	3.165	3.195 ± 0.024
11	1:1000	6	4	50	3.262	3.212 ± 0.024
12	1:400	6	3	40	3.517	3.524 ± 0.032
13	1:571	5	4	30	3.307	3.325 ± 0.026
14	1:571	6	5	30	3.599	3.659 ± 0.021
15	1:1000	5	4	40	3.471	3.527 ± 0.033
16	1:571	6	4	40	3.921	3.869 ± 0.046
17	1:1000	6	4	30	3.236	3.157 ± 0.023
18	1:400	6	4	50	3.743	3.681 ± 0.019
19	1:571	5	3	40	3.279	3.296 ± 0.034
20	1:571	6	4	40	3.921	4.025 ± 0.028
21	1:571	7	5	40	3.580	3.423 ± 0.025
22	1:400	6	5	40	4.328	4.381 ± 0.021
23	1:1000	6	3	40	3.291	3.284 ± 0.021
24	1:571	6	4	40	3.921	3.840 ± 0.037
25	1:571	6	4	40	3.921	3.924 ± 0.044
26	1:400	5	4	40	3.894	3.947 ± 0.029
27	1:571	6	4	40	3.921	3.946 ± 0.022
28	1:571	5	5	40	3.888	3.790 ± 0.009
29	1:571	7	3	40	3.086	3.044 ± 0.023

Note. Data are presented as mean ± S.D., where n=3; A = E/S ratio, B = pH, C = Reaction time, D = Temperature

The computed F-value (26.61) surpasses the tabulated F-value ($F_{14,14,0.05}$=2.48), demonstrating that the model is significant and shows strong agreement between the model and the experimental data [31]. This large F-value is statistically significant ($p < 0.0001$), as its probability of occurring by chance is exceptionally low. Furthermore, the p-value of this model ($p < 0.0001$) indicated that the model is statistically significant with a 95% confidence level [32]. The tabulated F-value ($F_{10,4,0.05}$=5.96) is higher than the lack-of-fit F-value, which is 1.88, indicating the lack-of-fit is not significant relative to the pure error. The lack-of-fit p-value, 0.2850, exceeds the p-value of 0.05, further reinforcing its insignificance, as there is a 28.50% chance that a lack-of-fit F-value this large could occur due to noise. The model's ability to closely reflect the true relationship between the variables, coupled with the absence of substantial fitting errors, suggests its suitability and reliability for predictive purposes. In essence, a statistically insignificant lack-of-fit indicates a well-aligned model [33]. The model had a high coefficient of determination (R^2 = 0.9638) and adjusted R^2 (0.9276), indicating an acceptable relationship between predicted and observed values. The model is deemed acceptable when the differences between adjusted R^2 and predicted R^2 are less than 0.2 [34]. The predicted R^2 of 0.8181 and an adequate precision value of 19.0794 further support the model's predictive capability and its utility in navigating the experimental design space for optimization purposes.

Table 3 Regression coefficients and ANOVA for the quadratic polynomial models of TRS production

Source	Coefficients	Degree of Freedom	*F*-value	*p*-value	Remark
Model	3.92	14	26.61	< 0.0001	Significant
A	0.2426	1	83.93	< 0.0001	
B	-0.1250	1	22.29	0.0003	
C	0.2757	1	108.38	< 0.0001	
D	0.0108	1	0.1674	0.6886	
AB	0.0313	1	0.4665	0.5057	
AC	0.1294	1	7.96	0.0136	
AD	-0.0022	1	0.0022	0.9630	
BC	-0.0288	1	0.3949	0.5398	
BD	-0.0769	1	2.81	0.1157	
CD	0.0588	1	1.64	0.2209	
A^2	-0.0710	1	3.88	0.0688	
B^2	-0.2927	1	66.04	< 0.0001	
C^2	-0.1701	1	22.30	0.0003	
D^2	-0.3585	1	99.04	< 0.0001	
Residuals		14			
Lack of Fit	3.92	10	1.88	0.2850	Insignificant
Pure Error		4			
Total Correlation		28			
Statistical					
R^2	0.9638				
Adjusted R^2	0.9276				
Predicted R^2	0.8181				

Note. A = E/S ratio, B = pH, C = Reaction time, D = Temperature

E/S ratio, pH, and reaction time exhibited statistically significant effects among the linear terms ($p < 0.0001$, $p=0.0003$, and $p < 0.0001$, respectively), demonstrating the importance they play in influencing the efficiency of TRS yields. Because of that, finding optimal conditions of those parameters, which are the E/S ratio, pH, and reaction time, played a very important role in ensuring overall hydrolysis efficiency, maintaining structural integrity,

and maximizing production of yields [35]. On the other hand, it was discovered that the linear influence of temperature was not particularly significant (p=0.6886). A notable two-way interaction was identified between E/S ratio and time (p=0.0136), indicating that the influence of one factor on hydrolysis yield depends on the degree of the other. This aligns well with findings from studies that utilize RSM, which emphasizes the significance of interaction among extraction variables [36]. The quadratic terms for pH, reaction time, and temperature were significant ($p < 0.0001$, p=0.0003, and $p < 0.0001$, respectively), showing non-linear interactions between these factors and the response variable. The quadratic term for the E/S ratio neared significance but did not attain the standard threshold (p=0.0688). From RSM analysis, the predicted response, reducing sugar, can be determined by following the second-order polynomial Equation (6):

$$\text{Total Reducing Sugar (mg/mL)} = 3.92 + 0.2425A - 0.1250B + 0.2757C + 0.0108D + 0.0313AB + 0.1294AC - 0.0022AD - 0.0288BC - 0.0769BD + 0.0588CD - 0.0710A^2 - 0.2927B^2 - 0.1701C^2 - 0.3585D^2 \quad (6)$$

The interaction between E/S ratio (A) and reaction time (C) is the most significant ($p < 0.05$) and demonstrates synergistic effect (Figure 5). When the E/S ratio is below 1:500 and the reaction time is shorter than 5 h, the hydrolysis remains incomplete. This is usually caused by insufficient enzyme availability to effectively hydrolyze glucomannan within a limited timeframe. Alternatively, simultaneously increasing both the E/S ratio and reaction time up to an optimal level (1:500 and 5 h, respectively) directly correlates with a substantial increase in reducing sugar yields. This is because a higher enzyme concentration provides more active sites for hydrolysis, while a prolonged reaction time allows for more complete glucomannan degradation [37]. This trend also aligns with previous findings, where both reducing sugar concentration and hydrolysis yield increased with rising enzyme concentrations across various hydrolysis times [37]. Other interaction terms (AB, AD, BC, BD, CD) were found to be not significant ($p > 0.05$), indicating that these variables do not exhibit meaningful combined effects on reducing sugar yield. Instead, their contributions may independently affect reducing sugar yields. Similar observations were reported by Wang *et al*. [38], who noted that while various parameters, such as enzyme concentration and hydrolysis conditions, affect the quality of the resulting hydrolysate, certain interactions between these factors do not significantly influence the overall yield. Jiao *et al*. [39] also reported comparable trends in their optimization study on sweet potato starch, where the interaction between parameters such as α-amylase and transglucosidase concentrations was insignificant, indicating that certain enzymatic variables act independently rather than cooperatively.

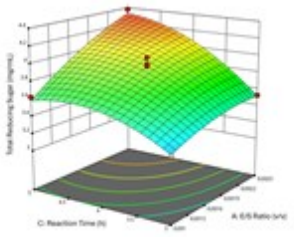

Figure 5 Response surface plots for the interaction between E/S ratio and reaction Time

3.7 Validation of the model

For the RSM solutions to achieve maximum TRS yields, the other parameters were set within range, and the response (TRS) was set at maximum. Table 4 presents the validation result of RSM models, which illustrates strong agreement between the expected and experimental value of reducing sugar with an error percentage of 1.46%. An error under 5% is often considered acceptable for model validation, especially in bioprocessing studies, as it indicates a strong concordance between predicted and experimental values [40]. The experimental yield of 4.409 ± 0.030 mg/mL closely matches the anticipated value of 4.343 mg/mL, suggesting the robustness and reliability of the RSM model in optimizing the enzyme hydrolysis process under specified conditions (E/S ratio 1:500 (v/v), pH 5.7, 5 h, and 41.5 °C). The small difference between the expected and observed values implies the model's accuracy in identifying the relationship between the input parameters and reducing sugar yields. The validation proves the suitability of the RSM methods for foreseeing and optimizing operating conditions of extraction methods.

Table 4 Expected and experimental results of reducing sugar yields

Parameter				Actual Reducing Sugar (mg/mL)	Expected Reducing Sugar (mg/mL)	Error %
E/S Ratio (v/v)	pH	Time (h)	Temperature (°C)			
1:500	5.7	5	41.5	4.409 ± 0.030	4.345	1.46

4.0 CONCLUSION

The study demonstrated that glucomannan derived from *Amorphophallus muelleri* can be efficiently hydrolyzed into oligosaccharides utilizing β-mannanase. To systematically evaluate the factors affecting hydrolysis performance, the effects of E/S ratio, pH, reaction time, and temperature were assessed. Initial OFAT screening revealed that the highest total reducing sugar (TRS) yield, 3.868 mg/mL,

was obtained under an E/S ratio of 1:500, pH 6, a temperature of 40 °C, and a reaction time of 4 h. Building on these preliminary findings, RSM optimization identified slightly adjusted but more effective conditions. The optimized conditions for hydrolysis (a 1:500 E/S ratio, pH 5.7, temperature 41.5 °C, and a reaction time of 5 h) resulted in 4.409 ± 0.030 mg/mL of total reducing sugars, which closely aligned with the model's predicted output, with a deviation of only 1.46%. Overall, among the variables studied, the enzyme-substrate (E/S) ratio, pH, and reaction time had significant influence on the reducing sugar yields, while temperature exhibited a minimal effect. Moreover, the RSM approach successfully enhanced the maximum yield of TRS by approximately 14% compared to the screening results, highlighting the effectiveness of statistical optimization in improving enzymatic hydrolysis performance. Collectively, these findings indicate the potential of *A. muelleri* as a promising and unexploited source of functional oligosaccharides. Its capacity to produce high yields of bioactive hydrolysis products suggests promising applications in food, and health-related industries.

Acknowledgements

The authors acknowledge the financial support from Ministry of Higher Education, Malaysia and Universiti Teknologi Malaysia under the Geran Penyelidikan Hi-Tech(F4+) 2024 (Q.J130000.4609.00Q37), as well as the Professional Development Research University Grant (R.J130000.7113.07E91), where Nur Aizura Mat Alewi is a Post Doctoral Fellow of Universiti Teknologi Malaysia.

Conflicts of Interest

The authors declare that there is no conflict of interest regarding the publication of this paper.

References

[1] Pambudi, A. Y., Harijati, N., and Arumingtyas, E. L. 2020. Physiological and Genetic Variations of *Amorphophallus variabilis* in Bojonegoro Based on Glucomannan Content, Calcium Oxalate and RAPD Markers. *The Journal of Experimental Life Sciences*. 10(1): 49–54. https://doi.org/10.21776/ub.jels.2019.010.01.09.

[2] Mekkerdchoo, O., Borompichaichartkul, C., Perrigo, A. L., Srzednicki, G., Prakitchaiwattana, C., and Antonelli, A. 2016. Tracing the Evolution and Economic Potential of Konjac Glucomannan in *Amorphophallus* Species (*Araceae*) using Molecular Phylogeny and RAPD Markers. *Phytotaxa*. 282(2): 81–106. https://doi.org/10.11646/phytotaxa.282.2.1.

[3] Tarigan, N., Tarigan, F. N., Sherlina, S., Hasibuan, Y. O., and Saragih, M. 2024. Sensory Test and Proximate Analysis Content Test of Porang Flour (*Amorphophallus muelleri*) and Tempe Flour Flakes. *Amerta Nutrition*. 8(2): 230–238. https://doi.org/10.20473/amnt.v8i2.2024.230-238.

[4] Nugrahaeni, N., Hapsari, R. T., Trustinah, Indriani, F. C., Sutrisno, Amanah, A., Yusnawan, E., Mutmaidah, S., Baliadi, Y., and Utomo, J. S. 2021. Morphological Characteristics of Madiun 1, the First Porang (*Amorphophallus muelleri* Blume) Released Cultivar in Indonesia. *IOP Conference Series: Earth and Environmental Science*. 911(1): 012011. https://doi.org/10.1088/1755-1315/911/1/012011.

[5] Chen, H., Nie, Q., Hu, J., Huang, X., Yin, J., and Nie, S. 2021. Multiomics Approach to Explore the Amelioration Mechanisms of Glucomannans on the Metabolic Disorder of Type 2 Diabetic Rats. *Journal of Agricultural and Food Chemistry*. 69(8): 2632–2645. https://doi.org/10.1021/acs.jafc.0c07871.

[6] Ariestanti, C. A., Seechamnanturakit, V., Harmayani, E., and Wichienchot, S. 2019. Optimization on Production of Konjac Oligo-glucomannan and Their Effect on the Gut Microbiota. *Food Science & Nutrition*. 7(2): 788–796. https://doi.org/10.1002/fsn3.927.

[7] Ashaolu, T. J., Ashaolu, J. O., and Adeyeye, S. A. O. 2021. Fermentation of Prebiotics by Human Colonic Microbiota In Vitro and Short-chain Fatty Acids Production: A Critical Review. *Journal of Applied Microbiology*. 130(3): 677–687. https://doi.org/10.1111/jam.14843.

[8] Ağagündüz, D., Özata-Uyar, G., Kocaadam-Bozkurt, B., Özturan-Şirin, A., Capasso, R., Al-Assaf, S., and Özoğul, F. 2023. A Comprehensive Review on Food Hydrocolloids as Gut Modulators in the Food Matrix and Nutrition: The Hydrocolloid-gut-health Axis. *Food Hydrocolloids*. 145: 109068. https://doi.org/10.1016/j.foodhyd.2023.109068.

[9] Li, K., Qi, H., Liu, Q., Li, T., Chen, W., Li, S., Piao, H., and Yin, H. 2020. Preparation and Antitumor Activity of Selenium-modified Glucomannan Oligosaccharides. *Journal of Functional Foods*. 65: 103731. https://doi.org/https://doi.org/10.1016/j.jff.2019.103731.

[10] Wang, H., Lai, C., Tao, Y., Zhou, M., Tang, R., and Yong, Q. 2023. Evaluation of the Enzymatic Production and Prebiotic Activity of Galactomannan Oligosaccharides Derived from Gleditsia Microphylla. *Fermentation*. 9(7): 632. https://doi.org/10.3390/fermentation9070632.

[11] Sun, Y., Chen, X., Cheng, Z., Liu, S., Yu, H., Wang, X., & Li, P. (2017). Degradation of Polysaccharides from *Grateloupia filicina* and Their Antiviral Activity to Avian Leucosis Virus Subgroup J. *Marine Drugs*. 15(11): 345. https://doi.org/10.3390/md15110345

[12] Mora, L., and Toldrá, F. 2023. Advanced Enzymatic Hydrolysis of Food Proteins for the Production of Bioactive Peptides. *Current Opinion in Food Science*. 49: 100973. https://doi.org/10.1016/j.cofs.2022.100973.

[13] de Mello Capetti, C. C., Dabul, A. N. G., Pellegrini, V. de O. A., and Polikarpov, I. 2023. Mannanases and Other Mannan-degrading Enzymes. In Glycoside Hydrolases (pp. 279–293). Elsevier. https://doi.org/10.1016/B978-0-323-91805-3.00013-7.

[14] Tripetch, P., Lekhavat, S., Devahastin, S., Chiewchan, N., and Borompichaichartkul, C. 2023. Antioxidant Activities of Konjac Glucomannan Hydrolysates of Different Molecular Weights at Different Values of pH. *Foods*. 12(18): 3406. https://doi.org/10.3390/foods12183406.

[15] Pomsang, P., Ayuni, D., Phumsombat, P., Eugelio, F., Fanti, F., Compagnone, D., and Borompichaichartkul, C. 2024. Enzymatic Hydrolysis and Biological Activities of Konjac Glucomannan Hydrolysate in Different Degree of Polymerisation. *International Journal of Food Science & Technology*. 59(11): 8341–8350. https://doi.org/10.1111/ijfs.17548.

[16] Araújo, N. G., da Silva, J. B., Moreira, R. T., and Cardarelli, H. R. 2021. Effect of Temperature and Concentration of βeta-galactosidase on the Composition of Reduced Lactose Pasteurized Goat Milk. *Food Science and Technology*. 41(2): 432–438. https://doi.org/10.1590/fst.05220.

[17] AOAC. 1995. Official Methods of Analysis (16th ed.). Arlington, Virginia, USA: Association of Official Analytical Chemists.
[18] Chua, M., Chan, K., Hocking, T. J., Williams, P. A., Perry, C. J., and Baldwin, T. C. 2012. Methodologies for the Extraction and Analysis of Konjac Glucomannan from Corms of *Amorphophallus konjac K. Koch*. *Carbohydrate Polymers*. 87(3): 2202–2210. https://doi.org/10.1016/j.carbpol.2011.10.053.
[19] Bradford, M. M. 1976. A Rapid and Sensitive Method for the Quantitation of Microgram Quantities of Protein Utilizing the Principle of Protein-dye Binding. *Analytical Biochemistry*. 72(1): 248c254. https://doi.org/https://doi.org/10.1016/0003-2697(76)90527-3.
[20] Miller, G. L. 1959. Use of Dinitrosalicylic Acid Reagent for Determination of Reducing Sugar. *Analytical Chemistry*. 31(3): 426–428. https://doi.org/10.1021/ac60147a030.
[21] Nur'aini, D. I., & Setiawan, A. A. 2020. Macronutrients Analysis of Porang Tubers (Amorphophallus muelleri Blume) Fermentation with Lactobacillus Bulgaricus Bacteria. *ICoSIHSN*. 33: 488-492 https://doi.org/10.2991/ahsr.k.210115.096
[22] Anggela, A., Setyaningsih, W., Wichienchot, S., and Harmayani, E. 2021. Oligo-glucomannan Production from Porang (*Amorphophallus oncophyllus*) Glucomannan by Enzymatic Hydrolisis using β-Mannanase. *Indonesian Food and Nutrition Progress*. 17(1): 23–27. https://doi.org/10.22146/ifnp.57217
[23] Li, H., Yang, J., Qin, A., Yang, F., Liu, D., Li, H., and Yu, J. 2022. Milk Protein Hydrolysates Obtained with Immobilized Alcalase and Neutrase on Magnetite Nanoparticles: Characterization and Antigenicity Study. *Journal of Food Science*. 87(7): 3107–3116. https://doi.org/10.1111/1750-3841.16189
[24] Yin, J.-Y., Ma, L.-Y., Xie, M.-Y., Nie, S.-P., and Wu, J.-Y. 2020. Molecular Properties and Gut Health Benefits of Enzyme-hydrolyzed Konjac Glucomannans. *Carbohydrate Polymers*. 237: 116117. https://doi.org/https://doi.org/10.1016/j.carbpol.2020.116117.
[25] Zu, X., Huang, Y., Zhao, Y., Xiong, G., Liao, T., and Li, H. 2023. Peptide Extraction from Silver Carp (Hypophthalmichthys molitrix) Scales via Enzymatic Hydrolysis and Membrane Filtration. *Italian Journal of Food Science*. 35(2): 44–53. https://doi.org/10.15586/ijfs.v35i2.2248.
[26] Suzuki, K., Michikawa, M., Sato, H., Yuki, M., Kamino, K., Ogasawara, W., Fushinobu, S., and Kaneko, S. 2018. Purification, Cloning, Functional Expression, Structure, and Characterization of a Thermostable β-mannanase from *Talaromyces trachyspermus* B168 and Its Efficiency in Production of Mannooligosaccharides from Coffee Wastes. *Journal of Applied Glycoscience*. 65(2): 13–21. https://doi.org/10.5458/jag.jag.JAG-2017_018.
[27] Sui, W., Liu, X., Sun, H., Li, C., Parvez, A. M., and Wang, G. 2021. Improved High-Solid Loading Enzymatic Hydrolysis of Steam Exploded Corn Stalk using Rapid Room Temperature γ-valerolactone Delignification. *Industrial Crops and Products*. 165: 113389. https://doi.org/10.1016/j.indcrop.2021.113389.
[28] Goemaere, I., Punj, D., Harizaj, A., Woolston, J., Thys, S., Sterck, K., De Smedt, S. F., De Vos, W. H., and Braeckmans, K. 2023. Response Surface Methodology to Efficiently Optimize Intracellular Delivery by Photoporation. *International Journal of Molecular Sciences*. 24(4): 3147. https://doi.org/10.3390/ijms24043147.
[29] Choi, G.-H., Lee, N., and Paik, H. 2021. Optimization of Medium Composition for Biomass Production of *Lactobacillus plantaru* 200655 using Response Surface Methodology. *Journal of Microbiology and Biotechnology*. 31(5): 717–725. https://doi.org/10.4014/jmb.2103.03018.
[30] Basri, M. S. M., Mustapha, F., Mazlan, N., and Ishak, M. R. 2021. Rice Husk Ash-Based Geopolymer Binder: Compressive Strength, Optimize Composition, FTIR Spectroscopy, Microstructural, and Potential as Fire-Retardant Material. *Polymers*. 13(24): 4373. https://doi.org/10.3390/polym13244373
[31] Kahar, I. N. S., Othman, N., Idrus-Saidi, S. A., Noah, N. F. M., Nozaizeli, N. D., and Suliman, S. S. 2024. Integrated Emulsion Liquid Membrane Process for Enhanced Silver Recovery from Copper-Silver Leached Solution. *Chemical Engineering Research and Design*. 212: 434–444. https://doi.org/10.1016/j.cherd.2024.11.018.
[32] Fetimi, A., Dâas, A., Benguerba, Y., Merouani, S., Hamachi, M., Kebiche-Senhadji, O., and Hamdaoui, O. 2021. Optimization and Prediction of Safranin-O Cationic Dye Removal from Aqueous Solution by Emulsion Liquid Membrane (ELM) using Artificial Neural Network-Particle Swarm Optimization (ANN-PSO) Hybrid Model and Response Surface Methodology (RSM). *Journal of Environmental Chemical Engineering*. 9(5): 105837. https://doi.org/https://doi.org/10.1016/j.jece.2021.105837.
[33] Jamaludin, R., Kim, D.-S., Md Salleh, L., and Lim, S.-B. 2020. Optimization of High Hydrostatic Pressure Extraction of Bioactive Compounds from Noni Fruits. *Journal of Food Measurement and Characterization*. 14: 2810–2818. http://dx.doi.org/10.1007/s11694-020-00526-w.
[34] Thakur, A., and Jawa, G. K. 2022. Screening of Parameters and Optimization for Green Recovery of Anionic Dye by Nanoparticle-Ionic Liquid-Based Green Emulsion Liquid Membrane using Response Surface Methodology. *Chemical Engineering and Processing-Process Intensification*. 181: 109156. https://doi.org/10.1016/j.cep.2022.109156.
[35] Fawale, O. S., Mudgil, P., Abdelrahman, R., Baba, W. N., Nirmal, N. P., and Maqsood, S. 2022. Anti-hypercholesteraemic and Antioxidative Activities of Camel Skin Gelatin Hydrolysate: Effect of Enzyme Type, Enzyme:Substrate Ratio and Time of Hydrolysis. *International Journal of Food Science & Technology*. 58(4): 2151–2160. https://doi.org/10.1111/ijfs.16224.
[36] Li, Y., Cao, S., Lin, S.-J., Zhang, J., Gan, R., and Li, H. 2019. Polyphenolic Profile and Antioxidant Capacity of Extracts from *Gordonia axillaris* Fruits. *Antioxidants*. 8(6): 150. https://doi.org/10.3390/antiox8060150.
[37] Putri, D. N., Perdani, M. S., Yohda, M., Utami, T. S., Sahlan, M., and Hermansyah, H. 2021. Effect of Ultrasound-assisted on Sequential Peracetic Acid and Alkaline Peroxide Pretreatment to the Enzymatic Hydrolysis of Oil Palm Empty Fruit Bunch. https://doi.org/10.21203/rs.3.rs-284744/v1.
[38] Wang, X., Yu, H., Xing, R., Liu, S., Chen, X., and Li, P. 2020. Optimization of Oyster (*Crassostrea talienwhanensis*) Protein Hydrolysates using Response Surface Methodology. *Molecules*. 25(12): 2844. https://doi.org/10.3390/molecules25122844.
[39] Jiao, Y., Wang, P., Niu, L., Ai, R., Xin, L., Song, A., Yang, G., & Zhang, K. 2025. Optimization of Enzymatic Parameters for Enhancing Branch Density and Flow Properties of Sweet Potato Starch. *Food Science & Nutrition*, 13(9). https://doi.org/10.1002/fsn3.70822.
[40] Rajamanickam, V., Babel, H., Montano-Herrera, L., Ehsani, A., Stiefel, F., Haider, S., Presser, B., and Knapp, B. L. 2021. About Model Validation in Bioprocessing. *Processes*. 9(6): 961. https://doi.org/10.3390/pr9060961.